RevMexAA (Serie de Conferencias), **1**, 157-164 (1995)

FORMATION AND EARLY EVOLUTION OF PROTOSTELLAR DISKS

Peter Bodenheimer and Gregory Laughlin[1]
UCO/Lick Observatory, University of California, Santa Cruz, CA 95064, USA

RESUMEN

Con el fin de seguir el colapso de un núcleo molecular rotando con 1 $M_\odot$ hasta una configuración que consiste de una estrella central, un disco rodeándola y una envoltura cayendo hacia el centro, hemos realizado una serie de cálculos hidrodinámicos en dos dimensiones con difusión de radiación. El disco acrece masa hasta un punto donde se vuelve inestable gravitatoriamente a los modos de orden bajo. Los resultados que hemos obtenido en dos dimensiones se usan después como condiciones iniciales para los cálculos SPH de tres dimensiones, con el fin de seguir la evolución no axesimétrica. Se desarrollan ondas espirales de densidad, con una transferencia de masa hacia adentro y momento angular hacia afuera. El reajuste del perfil de densidad de superficie implica una evolución hacia configuraciones que son gravitatoriamente estables. El tiempo de escala en que opera la inestabilidad se estima en unos pocos 10^5 años. Los resultados de esos cálculos indican que los discos inestables gravitatoriamente que se hayan formado del colapso de una nube transferirán la mayoría de su materia hacia la estrella central y, por tanto, es improbable que se forme una compañera binaria por fragmentación.

ABSTRACT

Two dimensional hydrodynamic calculations with radiation diffusion are employed to follow the collapse of a rotating molecular cloud core of 1 $M_\odot$ to a configuration consisting of a central star, a surrounding disk, and the remaining infalling envelope. The disk accretes mass to the point where it becomes gravitationally unstable to low-order modes. The two-dimensional results are then used as initial conditions for three-dimensional SPH calculations to follow the non-axisymmetric evolution. Spiral density waves develop, resulting in the transfer of mass inward and angular momentum outward. The readjustment of the surface density profile results in evolution toward gravitationally stable configurations; the timescale over which the instability operates is estimated to be several times 10^5 yr. A further calculation is presented for the collapse of a 10 $M_\odot$ clump, which also results in an unstable disk. The results of these calculations strongly indicate that a gravitationally unstable disk formed from cloud collapse will transfer much of its matter onto the central star; it is unlikely that it will form a binary companion by fragmentation.

Key words: **HYDRODYNAMICS — ISM: CLOUDS — INFRARED: GENERAL — ACCRETION, ACCRETION DISKS**

1. INTRODUCTION

This paper discusses the gravitational collapse of rotating protostars of 1 and 10 $M_\odot$, the formation of disks in the central regions, and the evolution of the disk as a consequence of gravitational instability. The numerical calculation of the collapse and disk formation employs an axisymmetric two-dimensional hydrodynamic code

[1]Now at National Astronomical Observatory, Mitaka 181, Tokyo, Japan

with radiation transfer in the diffusion approximation, while the gravitational instability is examined with several different techniques, including a three-dimensional SPH calculation, linearized two-dimensional modal calculations, and two-dimensional non-axisymmetric grid-based calculations in the disk plane.

Some important issues associated with this problem are as follows: First, what are the appropriate initial conditions for the formation of a star-disk system? Numerical and analytical considerations indicate that a centrally condensed configuration, with density distribution steeper than a power law $\rho \propto r^{-1}$ will not fragment but will collapse to a disk. Such distributions are consistent with observations of molecular cloud cores (Ward-Thompson et al. 1994), but this result leaves unresolved the question of how binary systems form. Second, what is the predicted appearance of the emergent spectrum during early phases of disk evolution? Detailed studies (Adams, Lada, & Shu 1987; Laughlin & Bodenheimer 1994) show that observed spectral energy distributions fit well with theoretical models of protostars. Third, what are the important mechanisms for angular momentum transport in disks, what are the time scales, and at what evolutionary stage is each dominant? If protostars start collapse with angular momenta in the observed range for molecular cloud cores, their disks will almost inevitably become gravitationally unstable soon after formation; this paper considers only the angular momentum transport as a result of gravitational torques. Fourth, can angular momentum transport generated by spiral waves at relatively low amplitude be approximated by an equivalent viscosity in a one-dimensional diffusion equation? Only a few detailed studies have been done, but the results indicate that the situation is more complex than it would seem at first glance. Fifth, what is the importance of radiation pressure in high mass protostars? Recent calculations (Yorke et al. 1995) indicate that it is not important at 10 $M_\odot$, but at only slightly higher masses it is expected to become very important. Sixth, what are the implications of the angular momentum transport processes with regard to planet formation in disks? In the early stages when the disk is gravitationally unstable, the evolution time of the disk is shorter than the formation time of giant planets; therefore the formation of such planets would have to occur at a later time. Seventh, when a disk becomes gravitationally unstable, does it fragment or is mass simply transferred onto the central object by the action of gravitational torques arising from relatively low-amplitude spiral waves? This question is further discussed below.

2. 1 $M_\odot$: COLLAPSE

The numerical solution of the hydrodynamical equations for the collapse and disk formation of a 1 $M_\odot$ protostar is described by Yorke et al. (1993). Axisymmetry is assumed, and the finite-difference equations are solved on a set of nested grids, so that the spatial resolution is highest at the center of the protostar. The region interior to 2 AU is not resolved, and the accretion luminosity generated by the central protostellar core is calculated approximately. Radiation transport in the flux-limited diffusion approximation is calculated by an alternating-direction technique; Rosseland mean opacities from silicate, ice, and graphite grains are employed. The initial radius (R) is 4×10^{16} cm, the mean density is 8×10^{-18} g cm^{-3} with a distribution $\rho \propto r^{-2}$, the initial temperature is 20 K, and the specific angular momentum $j(R) = 7 \times 10^{20}$ cm^2 s^{-1}. With these parameters the initial ratio (α) of thermal to gravitational energy is 0.37, and the initial ratio (β) of rotational to gravitational energy is 0.01.

The results show that a very rapidly rotating unresolved stellar core of 0.5 $M_\odot$ is formed. The accretion onto this core provides most of the heating for the surrounding disk, which at an age of 10^5 yr has accumulated a mass of 0.5 $M_\odot$ and extends to a radius of 500 AU. The surrounding infalling dusty envelope has become optically thin in the polar direction, so that the pole-on and equator-on spectral energy distributions are significantly different, peaking at 30 and 75 μm, respectively. The density and velocity structure at the earlier time of 40,000 yr, where the disk becomes gravitationally unstable, is shown in Figure 1. Temperatures range from 500 K near the center to 30 K near the outer edge.

3. 1 $M_\odot$: GRAVITATIONAL INSTABILITY

The two-dimensional disk structure (shown in Fig. 1) as calculated from the axisymmetric collapse code at 40,000 yr is used as the initial condition for a three dimensional SPH calculation (Hernquist & Katz 1989). The SPH calculations use the "locally isothermal" approximation, in which each particle maintains its original temperature. This approximation is valid over times short enough so that a particle has not moved far from its original position and is consistent with the two-dimensional radiative transfer calculations. The initial minimum value of the Toomre Q in the disk was 1.3. Starting from random perturbations generated by the placement of 25,000 SPH particles, the simulation quickly developed a spiral mode pattern with strong components of

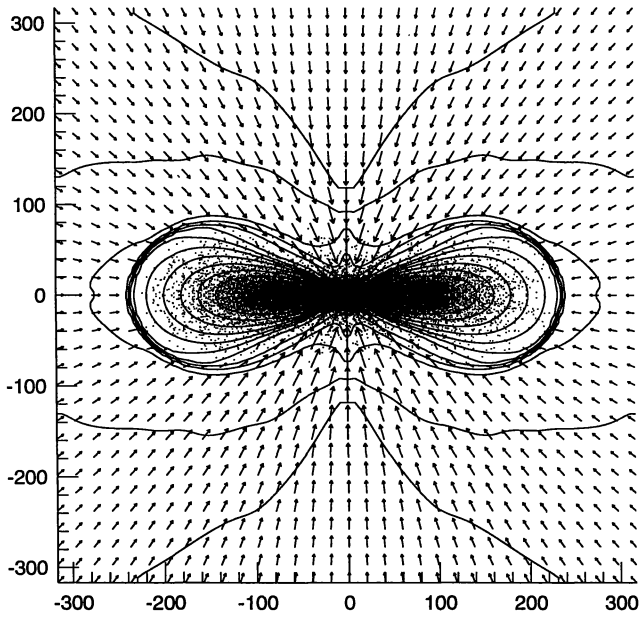

Fig. 1.— Density contours (solid lines) and velocity vectors (arrows) for the axisymmetric disk structure after 40,000 yr. Contours are separated by Δ log ρ = 0.2 with log ρ_{min} = −15.22. The length of the arrows is proportional to the speed, with a maximum value of about 5 km s^{-1}. The horizontal and vertical axes correspond to the equatorial plane and rotation axis, respectively; distances are marked in AU. Small dots mark the projected positions of the SPH particles at the onset of the 3-D calculation. From Laughlin & Bodenheimer (1994).

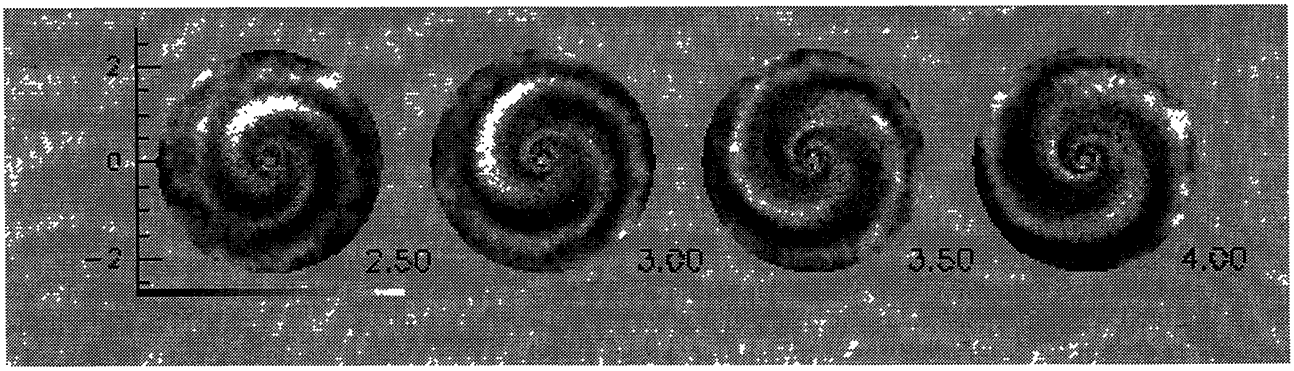

Fig. 2.— The surface overdensity distribution, defined as the ratio of the local surface density in the disk to the average surface density at that radius, at several times during the SPH evolution starting from the structure shown in Figure 1. The numbers at the lower right of each snapshot give the time in units of 477 yr. The gray-scale runs from 50% underdensity (black) to 50% overdensity (white). The radius of the disk in each case is 200 AU. Adapted from Laughlin & Bodenheimer (1994).

both $m = 1$ and $m = 2$. The calculation was run for 10 dynamical times, about 5000 yr, or several orbital periods at the position of minimum Q (100 AU). Examples of the spiral patterns are shown in Figure 2. Angular momentum transport and readjustment of the surface density profile towards stability, that is, toward higher Q, was the main feature of the results.

The evolutionary time scale of the disk whose evolution is shown in Figure 2 is estimated to be a few times 10^5 yr, somewhat shorter than that for a viscous disk with $\alpha = 0.01$. In fact, the redistribution of the surface density arising from the non-axisymmetric evolution has been compared (Laughlin & Bodenheimer 1994) with that obtained from the solution of the simple one-dimensional radial diffusion equation that describes the evolution of a thin disk (Lynden-Bell & Pringle 1974). The fit was quite good over a limited range in time, with an equivalent $\alpha = 0.03$. A further calculation with the SPH code was made, in which the temperature in the initial model was artificially reduced so that the minimum Toomre Q was 1.0. In this case an $m = 2$ spiral wave is excited, but the amplitude is much larger than that in the previous case, and the result seems to be fragmentation on a relatively short time scale. The result is shown in Figure 3. However it is questionable whether this initial condition could ever be reached as the result of the collapse of a protostar, because instability to the milder perturbations shown in Figure 2 occurs earlier in the evolution than instability to fragmentation. In both cases the instability appears to be driven by the broad surface density maximum near a radius of 80 AU, which is where Q attains its minimum.

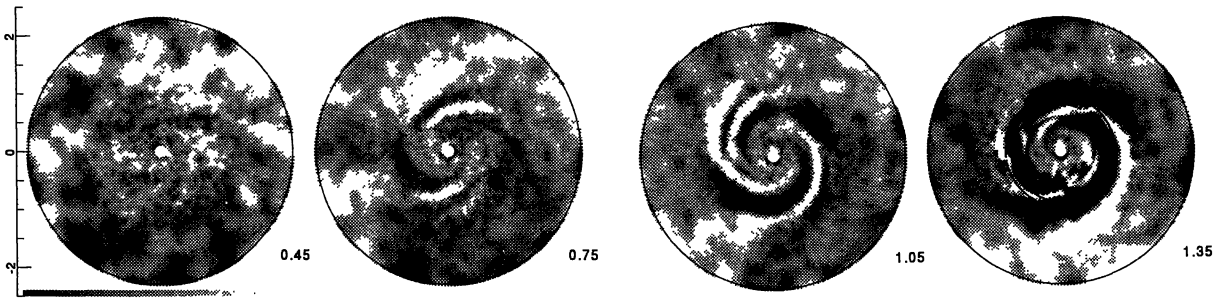

Fig. 3.— The surface overdensity distribution, defined as in Fig. 2, at several times during the SPH evolution starting from a structure with $Q_{min} = 1$. The numbers at the lower right of each snapshot give the time in units of 477 yr. The gray-scale runs from 200% underdensity (black) to 200% overdensity (white). The radius of the disk in each case is 200 AU. 12,500 particles were used in the simulation.

Further investigation of gravitational instability, with a view toward determining under which circumstances an equivalent α could be found, were undertaken with a two-dimensional grid-based code. Only the radial and azimuthal components of the equation of motion were taken into account, and the disk was assumed to have a polytropic equation of state. The inner boundary allows free accretion onto a central mass (M_*). An outer free Lagrangian condition is applied, so that the disk material is allowed to expand into an initially empty set of zones with outer radius twice the initial disk radius. A reflecting boundary condition was applied at the outer grid radius. The results from this code, with 128 radial and 128 azimuthal zones, were compared with those from linear simulations (Laughlin 1995) and with the non-linear calculations of Heemskerk, Papaloizou, & Savonije (1992); the agreement was excellent. The initial condition was a disk in equilibrium, extending from radii R_{in} to R_{out} with a Gaussian surface density profile – an approximation to the actual disk that results from collapse. The parameters are the Q_{min} in the disk and the initial ratio (R_m) of the disk mass to the total mass, $M_{disk}/(M_{disk} + M_*)$. An initial random perturbation in surface density was applied, with maximum amplitude $\pm$ 0.1%. An example of the results is shown in Figure 4. These calculations show an early phase during which the dominant mode arises from the random perturbation, then the linear development of the dominant two-armed spiral (Figure 4), and then a saturation of the amplitude after about 8 dynamical times.

A one-dimensional viscous diffusion calculation starting from the same initial density profile showed that the fit with a constant α was not particularly good; the α disk tends to evolve towards constant surface density σ. A better fit, shown in Figure 5, was obtained if α was assumed to vary as a function of radius, with the form $\alpha_{eff} = 0.225\sigma^{-1}\omega^{-0.8}$, where ω is the angular velocity. Further two- dimensional calculations were carried out, for the same Q_{min}, with R_m in the range 0.2 – 0.6. In all cases, two-armed spiral patterns developed, similar to those shown in Figure 4, but the amplitudes saturated at earlier times, at about the same values, for the simulations with larger disk masses. The two-dimensional calculations were found to fit a one-dimensional diffusion calculation if α was calculated according to $\alpha_{eff} = \beta\sigma^{-1}\omega^{\xi}$, where both β and ξ varied as a function

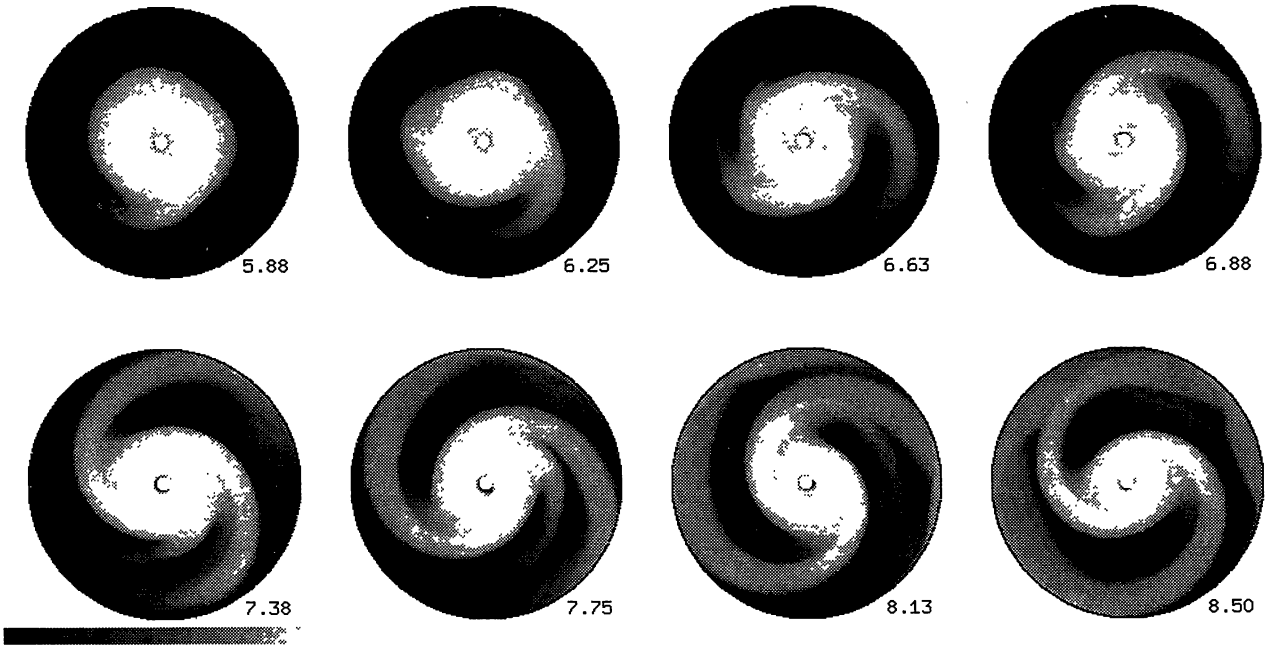

Fig. 4.— Evolution of the surface density distribution for a polytropic disk with initial $Q_{min} = 1.3$ and $R_m = 0.5$. Times on the lower right of each snapshot are given in units of π^{-1} times the orbital period at the outer edge of the grid. The logarithmic grayscale values run from log σ = -5.0 (dark) to log σ = 1.5 (light).

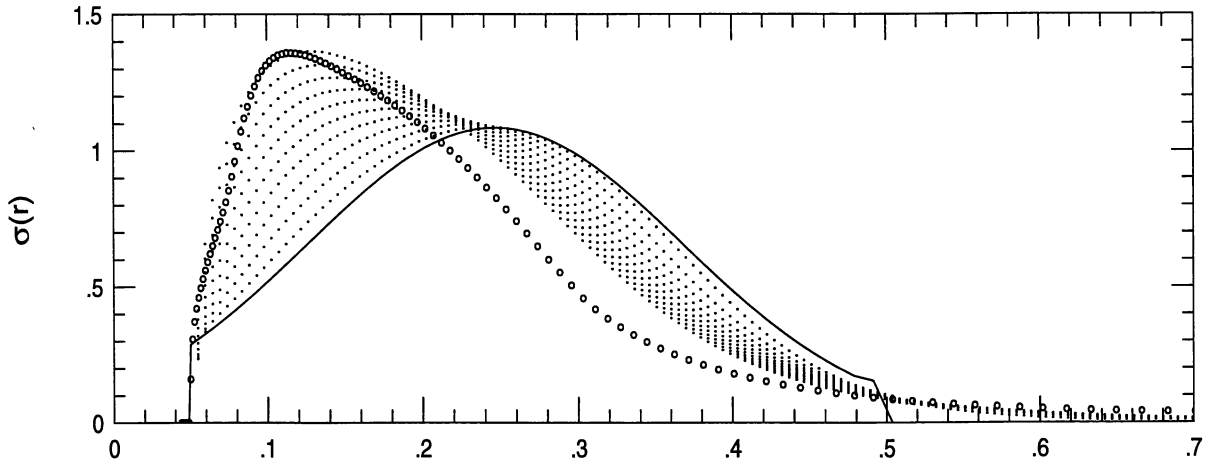

Fig. 5.— Azimuthally averaged surface density plotted as a function of radius (in units of the outer grid radius), for the calculation shown in Figure 4, at the initial time (solid line), and after 8.5 dynamical times (open circles). The small closed circles represent solutions to the one-dimensional radial diffusion equation with an α viscosity given by $\alpha_{eff} = 0.225\sigma^{-1}\omega^{-0.8}$, at equally-spaced time intervals up to 10.0 dynamical times.

of R_m. Therefore, the universal characterization of these evolutions, which were carried to longer times than that shown in Figure 2, in terms of an equivalent viscosity with constant α, appears not to be possible.

The "grand design" appearance of the two-armed spiral modes in these protostellar disks points to the underlying reason why the effective viscosity from gravitational torques is not well described by an α-prescription. An α-approximation is an attempt to treat the viscous evolution evoked by a *local* process such

as turbulence. However, the gravitational torques in the protostellar disks studied here arise from *long-range* forces exerted by the wide-open spirals. A WKB, or local, approximation to the perturbed potential is not valid here; hence it is natural that an α-model has difficulty in describing the long-term evolution of the surface density. A disk with a tightly-wound spiral pattern would presumably be more amenable to the α-prescription. However, to generate such a pattern the disk would have to be much less massive and much cooler than the disks found in our collapse calculations.

4. 10 $M_\odot$: COLLAPSE AND DISK EVOLUTION

A second calculation with the two-dimensional axisymmetric collapse code was performed for 10 $M_\odot$, outer radius 2×10^{16} cm, and initial uniform angular velocity $\Omega = 5 \times 10^{-12}$ s^{-1}, corresponding to a specific angular momentum of 2×10^{21} cm^2 s^{-1} at the outer edge. The density distribution, as in the 1 $M_\odot$ case, was $\rho \propto r^{-2}$. The unresolved central region had a radius of 2×10^{13} cm. Four nested grids were used, with 124 by 124 zones each. The results after 7000 years are shown in Figure 6. The unresolved core contains 2.7 $M_\odot$ at this time. Note the two accretion shocks on the surface of the disk, one of which encases the entire structure, and the second of which is evident closer to the disk surface, interior to 100 AU.

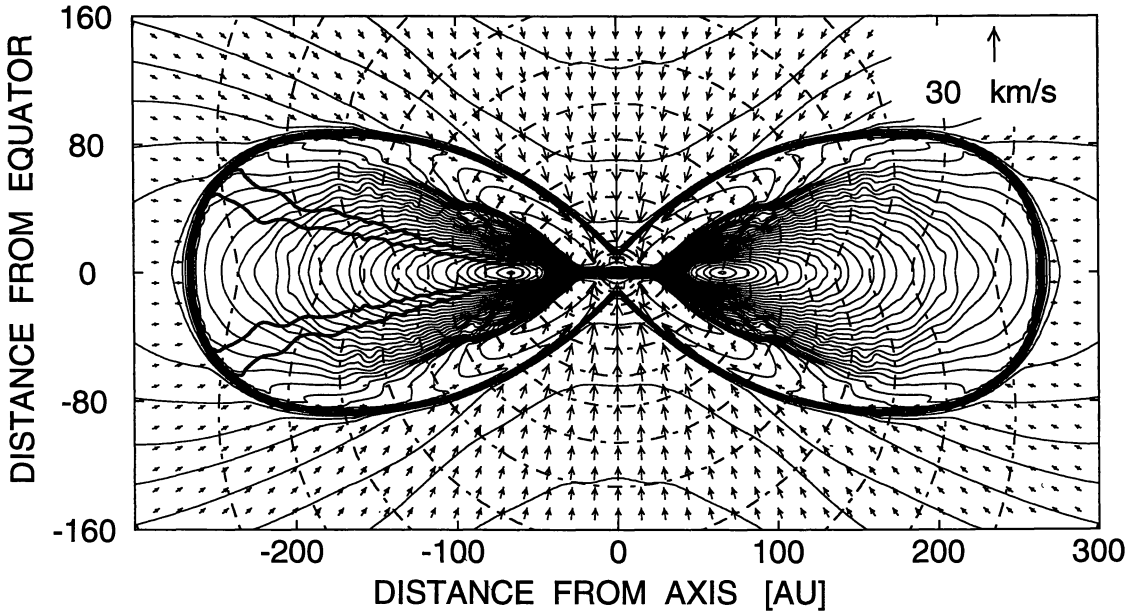

Fig. 6.— Density (solid lines) and temperature (dot-dashed lines) contours in the (R, Z) plane 7074 years after the onset of collapse of a 10 $M_\odot$ cloud fragment (Yorke, Bodenheimer, & Laughlin 1995). Contour intervals are Δ log ρ = 0.2 and Δ log T = 0.05. The two pairs of solid lines on the left half of the equilibrium disk correspond to $\pm$ 1 and 2 density scale heights above the equator.

There are several sharp ringlike density maxima in the midplane of the disk within 75 AU of the origin, indicating that the disk is gravitationally unstable at this time; the Q values at the maxima also indicate instability. To confirm this, the two-dimensional structure of the inner disk was fed into a three-dimensional SPH code with 2000 particles. On a very short time scale the axisymmetric ring structures broke up into small fragments (Fig. 7). These simulations demonstrate that there is a gravitational instability, but they do not represent the realistic evolution of the disk. In fact the gravitational instability would have set in at an earlier time in the disk formation and probably would have resulted in a spiral-arm instability of the type shown in Figure 2, rather than fragmentation. The estimated mass of the central object after the system has reestablished stability is $\approx$ 8 $M_\odot$, with the remaining 2 $M_\odot$ in the disk.

Figure 8 shows spectra of the 10 $M_\odot$ model at 7074 years, as a function of viewing angle. Clearly the infrared spectrum looks markedly different when viewed pole-on as compared to equator-on. In the polar direction, the

optical depth of infalling material has become sufficiently small so that the central star, which is assumed to have a surface temperature of 4800 K, becomes visible at wavelengths less than 1 μm. In the equator-on view only a single peak is present at 20 μm.

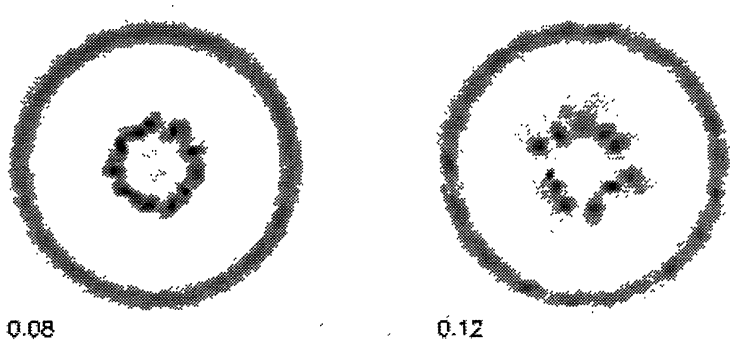

Fig. 7.— Surface density distributions of the inner part of the 10 $M_\odot$ disk after evolution with a 3–D SPH code, at two times which are given in units of the dynamical time of 44 yr. Darker regions correspond to higher densities. The radius of the outer ring is 25 AU. Adapted from Yorke et al. (1995).

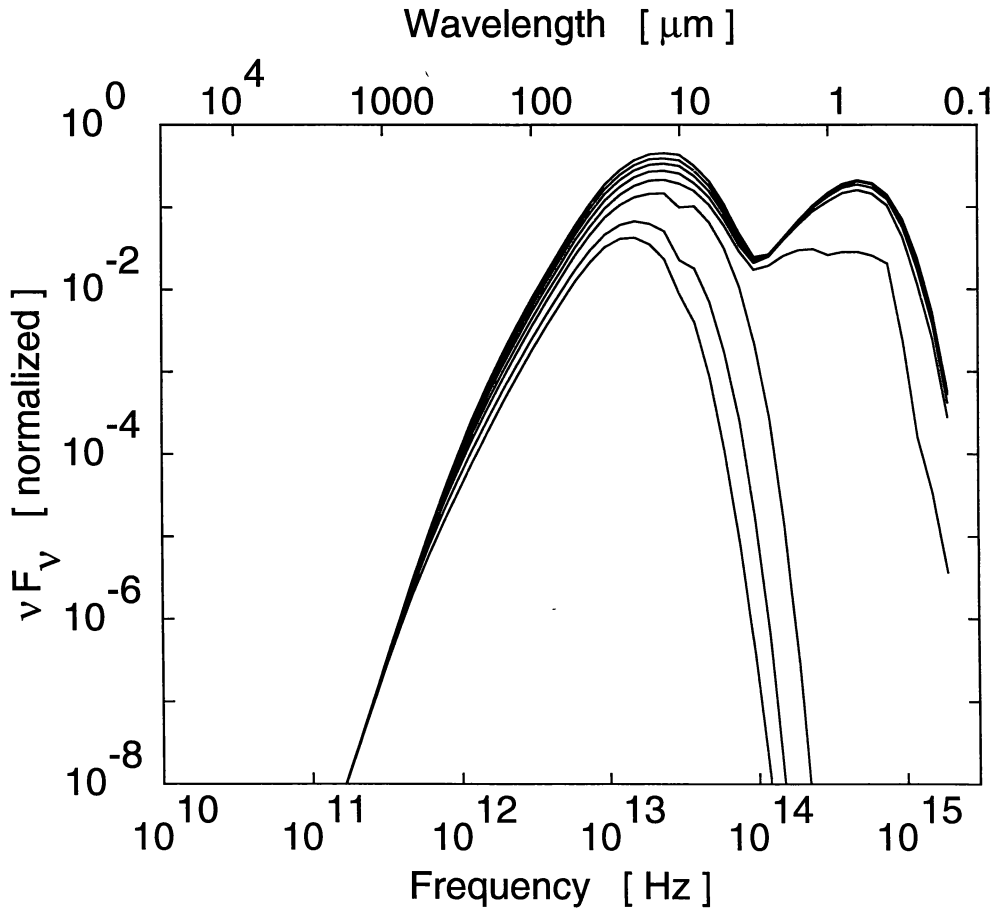

Fig. 8.— Spectra of the 10 $M_\odot$ protostar at 7074 yr as a function of viewing angle, plotted at equal intervals of cos θ, where $0 \leq \theta \leq 1$. The curve for θ =90° has the lowest maximum in νF_ν. From Yorke et al. (1995).

To summarize, the 10 $M_\odot$ protostar, after 7000 years of evolution, has a central core mass of 2.7 $M_\odot$. Its luminosity of 30 $L_\odot$ is supplied primarily by Kelvin-Helmholtz contraction rather than by accretion. It has a disk of about 7 $M_\odot$ with a radius of 260 AU and a midplane temperature range of 1500 to 150 K. It is gravitationally unstable in the region interior to 100 AU. An accretion shock, which is double in some regions, surrounds the equilibrium region at roughly 10 density scale heights above the midplane. Although radiative acceleration was included in the equations, this effect did not prevent collapse to a disk. The residual infalling envelope is optically thin along the rotation axis, but optically thick in dust in the equatorial plane, so that infrared spectral energy distributions would resemble those of Lada Class I objects or Lada Class II objects, when viewed in the equatorial and polar directions, respectively. The probable result of the gravitational instability, in this object as well as in the 1 $M_\odot$ case, is the transfer of much of the disk mass onto the central object. The details of the non-axisymmetric evolution for the 10 $M_\odot$ case, starting at the time when the disk first becomes gravitationally unstable, remain to be followed. In the collapse calculations, the value of Q_{min} (≈ 1.3) appropriate for the transfer of angular momentum by spiral waves in the disk occurs before the time that Q_{min} reaches 1.0, the value required for fragmentation to take place. Further detailed studies are required to determine whether in fact it is ever possible to reach a disk with $Q_{min} = 1$, with the possible resulting formation of a binary system, as the outcome of a protostar collapse.

REFERENCES

Adams, F. C., Lada, C., & Shu, F. H. 1987, ApJ, 312, 788
Heemskerk, M. H. M., Papaloizou, J. C., & Savonije, G. J. 1992, A&A, 260, 161
Hernquist, L., & Katz, N. 1989, ApJS, 70, 419
Laughlin, G. 1995, ApJ, submitted
Laughlin, G., & Bodenheimer, P. 1994, ApJ, 436, 335
Lynden-Bell, D., & Pringle, J. E. 1974, MNRAS, 168, 603
Ward-Thompson, D., Scott, P. F., Hills, R. E., & André, P. 1994, MNRAS, 268, 276
Yorke, H. W., Bodenheimer, P., & Laughlin, G. 1993, ApJ, 411, 274
Yorke, H. W., Bodenheimer, P., & Laughlin, G. 1995, ApJ, in press